UTILIZATION MAGNETIC FIELD AND RADIO FREQUENCY IDENTIFICATION FOR MOVING BLOCK SIGNALLING SYSTEM PROTOTYPE TO INCREASE LINE TRACK CAPACITY

Rifki Wijaya[1], Rahmat Siswanto[2], Ary Setijadi Prihatmanto[2], Ferry Stephanus Suwita[2], Reza Darmakusuma[2], Harits Ar Rosyid[3], Ardianto Satriawan[2] and Agus Sukoco[4]
[1]Department of Computer Engineering, Faculty of Electrical Engineering, Telkom University, Bandung, Indonesia
[2]Department of Electrical Engineering, Faculty of Electrical Engineering, Institut Teknologi Bandung, Bandung, Indonesia
[3]Department of Electrical Engineering, Faculty of Electrical Engineering, Universitas Negeri Malang, Malang, Indonesia
[4]Department of Computer Engineering, Faculty of Computer Science, Bandar Lampung University, Bandar Lampung, Indonesia
E-Mail: rifkiwijaya@telkomuniversity.ac.id

ABSTRACT

The line capacity of fixed block signaling is reciprocal of the minimum headway and is defined as the maximum number of the train that can pass through a stretch of track per unit time for safety reason. By using the Communication Based Train Control (CBTC) technology all trains continuously communicating their exact position. Therefore, the safety distance was no longer a static entity but an adjustable distance (moving block) based on a real-time calculation of the train speed. There will no longer wasted space so the line capacity will increase. The prototype form implemented in four sub-systems, the first one is signal generating system consisting of an oscillator circuit and amplifiers to generate AC signals and flow it to the loop cable produce electromagnetic waves, the signal processing sub-system which serves to read the oscillator signal on the loop cable by using the coil, data processing and communication sub-system processing signal output and send data to the server and the radio frequency identification as the wayside equipment for calibrating the position. The output of this implementation is sequence number of blocks that have been passed by the train and the information of the RFID tags used to calibrate the position of the train. By using that information, we can determine the position of the trains and kept the trains close to each other while maintaining a safety distance.

Keywords: cbtc, moving block, signaling, magnetic field, iot, rfid.

INTRODUCTION

Indonesia has finalized its plan for a national railway network. With more than 3,200km of train tracks that will crisscross the islands of Sumatra, Java, Kalimantan, and Sulawesi, it has been touted as the most extensive railway project in Indonesia according to Straits Times, 2017. The existing railway in Java and Sumatra has been serving for more than fifty years. The railway still using the traditional fixed block signaling for detecting the presence of a train. This signaling system has served the signaling community well over the past 150 years Naeem, *et al.,* 2015. The line capacity is reciprocal of the minimum headway and is defined as the maximum number of the train that can pass through a stretch of track per unit time Baheshti, *et al.,* 2003. But as major urban centers grow; the number of passengers increased every year. The train operator has two option build more subway lines or optimize their existing infrastructure by adopting new technologies Ali, *et al.,* 2015 to optimize headways between trains and increase line track capacity Yuan Cao, *et al.,* 2007 and Pochet, *et al.,* 2016. Optimize the existing infrastructure is more challenging because the operator has to achieve specified minimum time separation between trains (headway) while minimizing the amount of signaling equipment but maintaining the highest level of safety Khalifa, *et al.,* 2011.

The future of public transportation will consist of Realtime information, Big data for more precise resource allocation decisions and automation will be introduced in new circumstances that warrant it Zhao, *et al.,* 2009.

ANALYSIS AND SYSTEM DESIGN

Prototype design

Prototype form implemented on miniature electric train with scale 1:87 ratio due to the original train. Power supply give 12-volt electricity along the track and the train wheels forward it to train's motor.

There are four sub-system in this prototype, the first one is signal generating system consisting of an oscillator circuit and amplifiers to generate AC signals and flow it to the loop cable, the signal processing sub-system which serves to read the oscillator signal on the loop cable by using the coil, data processing and communication sub-system consists of a Wemos D1-mini an IoT device used for processing signal output and send data to the server, and the radio frequency identification as the wayside equipment for calibrating or check points. The block diagram of this prototype can be seen in Figure-1.

VOL. 15, NO. 5, MARCH 2020 ISSN 1819-6608
ARPN Journal of Engineering and Applied Sciences

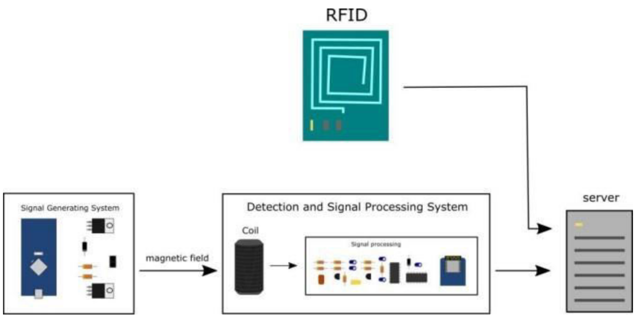

Figure-1. Diagram block of prototype.

The rail track layout of the train miniature is looping track with three loops in it as shown in the Figure-2.

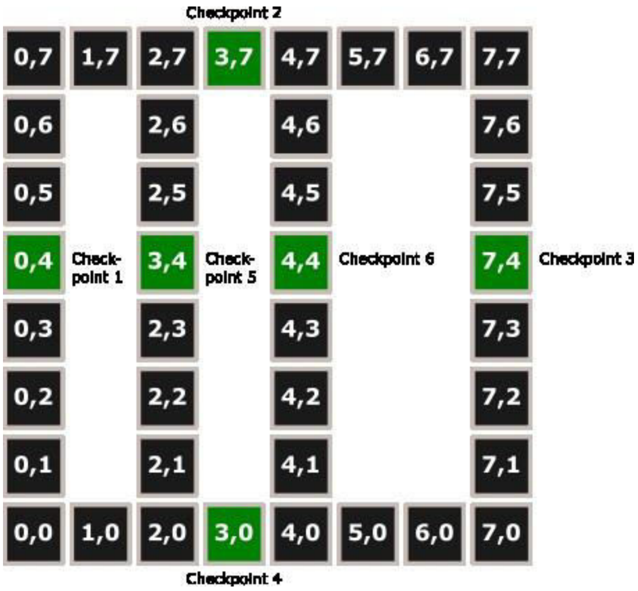

Figure-2. The layout of miniature rail track.

Each block represents the coordinate point with the x and y axes so the distance between trains can be easier to calculate with the following conditions:

- If the two trains are on the same axis on the track, the distance between trains is obtained using the Manhattan Distance formula as follows:

$$D = |x_1 - x_2| + |y_1 - y_2|$$

Where D is the distance of two trains, $x_1$is the x coordinate of train 1, $x_2$is the x coordinate of train 2, y_1 is the y coordinate of train 1 and y_2 is the y coordinate of train 2

- If one of the trains is on the inner lane, there are two formulas considered to determine the distance between trains.

$$D1 = (7 - y_1) + (7 - y_2) + |x_1 - x_2|$$

$$D2 = (y_1 + y_2) + |x_1 - x_2|$$

Determination of the use of the formula for the upper lane or the lower lane is by summing the *y* values of the two trains then compared with the maximum value of the axis *y* or equal to 7 in the prototype of this study. If the total value of the *y-axis* of the two trains is smaller than 7, the distance between trains is calculated using the formula of the distance of the upper train, if not then the formula for the distance of the lower lane train is used.

Signal generating system

The signal generating sub-system consists of two parts, the oscillator circuit, and the Loop cable. This sub-system produces magnetic fields derived from alternating current in the loop cable. Magnetic fields will be detected and processed by the sub-detection system and signal processing.

Arduino Nano used to generate an AC signal that will be streamed along the loop cable with 300 kHz frequency. The AC signal generated by the oscillator is connected to both ends of the loop cable. The signal generated by this oscillator will produce a magnetic field in the loop cable because of the alternating current flowing on the loop cable. To produce a square signal with a frequency of 300 kHz, the AVR timer feature is used with Clear Timer mode on Compare (CTC) Mode on Arduino nano Volinski, *et al.,* 2018.The illustration of this implementation can see in Figure-3.

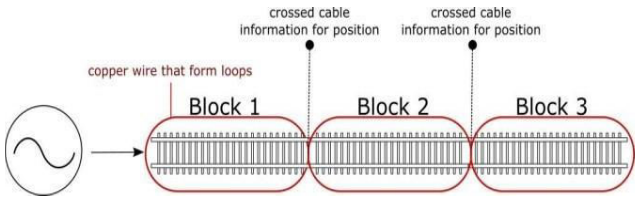

Figure-3. Illustration of streamed AC signal along the loop cable.

Figure-3 shows that signals which generated by an oscillator circuit streamed along the loop cables. Magnetic field more concentrated in the center of the loop than outside the loop as shown as Figure-4.

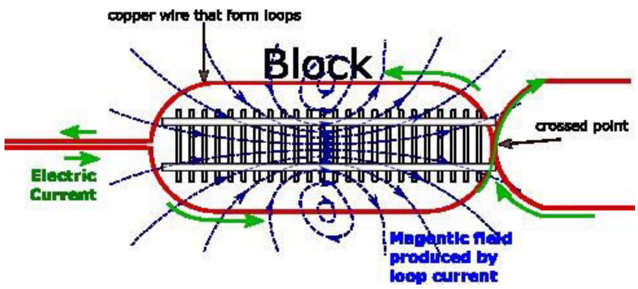

Figure-4. Magnetic field of current loop.

From Figure-4 each loops (blocks) transmit magnetic field inside them and shrink on the crossing point. This crossing point is the information that we will send to message broker.

Detection and signal processing system

The sub detection system and signal processor consist of two parts; the coil to detect magnetic fields emitted by loop cables and convert them into voltage signals, and the signal processing circuit. The coil specifications are as follows:

- The coil have 0.7 diameter
- The number of coil used is 260
- Diameter of cylindrical ferrite bars ± 2 cm
- Length of cylindrical ferrite bars is 6 cm

Figure-5. Coil.

The working principle of a coil based on Figure-5 is magnetically couple based on Faraday's law. According to Sirait, 2017, the magnetic field generated by the loop cable will produce alternating current which is converted to voltage in the coil. With the above specifications will get a large inductance by using the coil inductance formula on the solenoid as follows:

$$L = \frac{\mu \times N^2 \times A}{l}$$

With L = large inductance, μ = core permeability of the coil, N = number of turns, A = sectional area of the solenoid, and l = solenoid core length. The ferrite bar used as the core has a relative permeability of μ_r = 5, so the coil core permeability will be as follow:

$$\mu = \mu_r \times \mu_0$$

With μ_0 is the air core permeability of $4\pi\ x$ 10-7 Wb / Am, it will obtain a coil inductance value as follow.

$$L = \frac{\mu \times N^2 \times A}{l}$$

$$L = \frac{5 \times 4\pi \times 10^{-7} \times 260^2 \times \frac{\pi}{4} \times 0{,}02^2}{0{,}06}$$

$$L = 2{,}2\ \mathrm{mH}$$

The position of the coil must be inside the loop so the coil can detect the magnetic field which generated by the loop of the cable as shown as Figure-6.

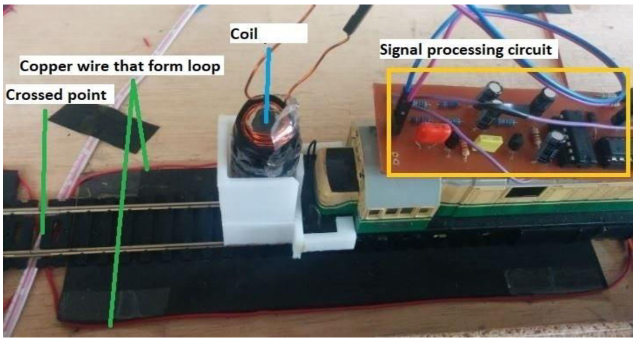

Figure-6. Position of coil and signal processing circuit on prototype.

The signal output will be read by wemos on analog port; if the coil position is inside the cable loop the value will greater than threshold because it detects the magnetic field and below that if the coil position is on the crossing point.

Communication system

The communication system plays as crucial role in the CBTC technology because all the information will send and receive by the communication devices. Radio CBTC system has become a trend for the development of metro. Many of WLAN standard technologies, including 802.11 FHSS, 802.11b DSSS, and 802.11 a&g OFDM, have already been applied to CBTC, Sree Harsha, *et al.*, 2016. The standard IEEE 802.11 WLAN, popularly known as Wi-Fi have used historically, mainly due to its cost-effectiveness Changqing, *et al.*, 2009. The prototype use Wemos D1mini, a microcontroller base on ESP8266, a low-cost Wi-Fi microchip with full TCP/IP stack. This device continuously sends all the information from the train. The data sent as a JSON string format to the message broker with structure as follows:

```
{
  "trainId": STRING,
  "position": STRING,
  "block": INTEGER,
  "speed": DOUBLE,
  "timestamp": STRING
}
```

JSON was chosen because it's easy to scalable and supported various languages. On the server side (at the station) the JSON string will be decoded into object data.

IMPLEMENTATION AND TESTING

Oscillator circuit consists of Arduino Nano, step down converter circuit, and also an amplifier that is placed on Arduino Nano output. The schematic of oscillator circuit can be seen in Figure-7.

VOL. 15, NO. 5, MARCH 2020 ISSN 1819-6608
ARPN Journal of Engineering and Applied Sciences

www.arpnjournals.com

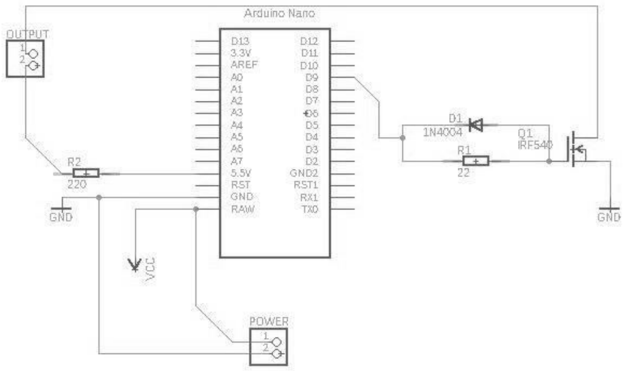

Figure-7. Schematic oscillator circuit.

From the Figure-7 the output current from Arduino Nano is only 40 mA that's why need to amplify so the to produce a strong magnetic field. Oscillator circuit and amplifiers to generate AC signals and flow it to the loop cable with ±5V peak-to-peak voltage (Vpp) and ±300 kHz frequency. By using oscilloscope, the output of this circuit can be seen in Figure-8.

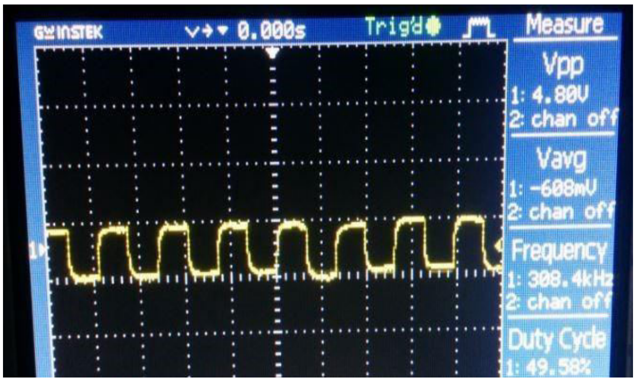

Figure-8. Output oscilloscope.

Figure-8 shows that the output of AC signal of oscillator is square signal, with 308kHz frequency and 4.80 Vpp. This is enough to produce a magnetic field. The signals of magnetic field will detect by coil then process them as in the schematic below.

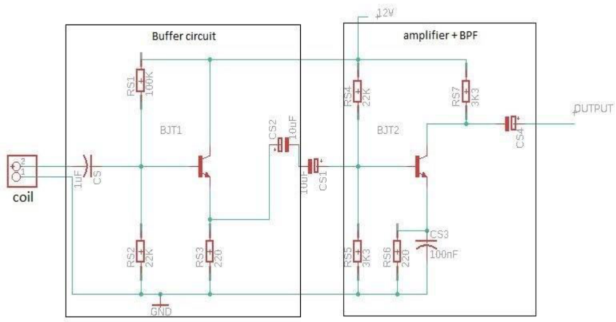

Figure-9. Schematic of buffer circuit and amplifier + BPF.

From Figure-9 the coil is used to detect magnetic fields emitted by loop cables and buffer circuit is used to forward the signal captured from the wire coil. The buffer circuit is needed as a reduction in errors that occur when the signal flows to the amplifier circuit due to a power load inside the amplifier. The small signal amplifier circuit with BPF is a circuit used to amplify the signal from the wire coil then need to add an IC Schmitt trigger to change the AC signal into a digital signal.

The coil detects the signal then the sub-system signal processing processes the signal into a digital value. The crossing point tested by running the train for 28 blocks with ±12 cm/s speed. The result of this test can be seen in Figure-10.

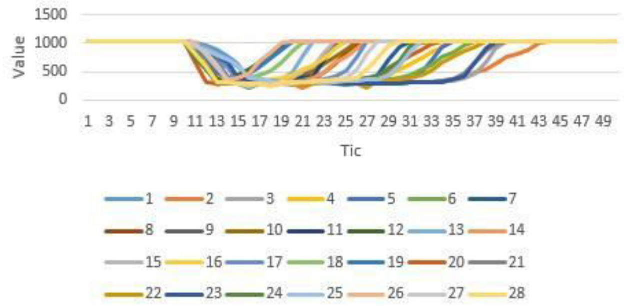

Figure-10. Output of Signal Processing Sub-system.

Base on the Figure-10 values are varied from 250 to 1024. When the coil inside the loop the value will be 1024 then shrink until 250 on the crossing point, that because the Wemos D1-Mini ADC resolution is a 10-bit ADC that can be detected up to 1024 (210) discrete analog levels. The threshold set to 700 because that is the median value between 250 and 1024.

The signal processing tested refer to the threshold value the test results can be seen in Figure-11 and Figure-12.

Figure-11. Signal value when coil inside the loop.

Figure-11 shows when the coil inside the loop, the value detects 1024, because it is above the threshold the Wemos does not publish any data to MQTT broker.

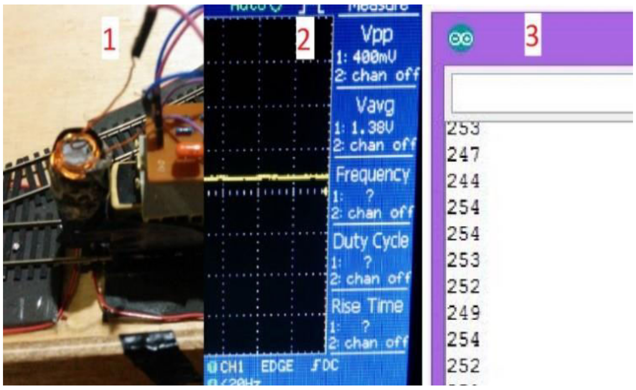

Figure-12. Signal value when the coil on the crossing point.

Figure-12 shows the value is ±252 when the coil on the crossing point because it is below the threshold the WEMOS publish JSON string to MQTT broker, the data contain speed and how many blocks the train has been passed.

The success rate of the train can detect the crossing point while running can see in the table below.

Table-1. Success rate of crossing point when the distance of the coil to center of the loop current is 1cm.

No	PWM (%)	Speed (cm/s)	Total crossing point	Fail detection	Success rate (%)
1.	10	4,61	28	0	100
2.	20	11,20	28	0	100
3.	30	17,71	28	0	100
4.	40	24,68	28	0	100
5.	50	31,41	28	1	96,42
6.	60	38,35	28	3	89,28
7.	70	43,81	28	6	78,58
8.	80	49,72	28	8	71,43
9.	90	58,85	28	11	60,72
10.	100	59,78	28	12	57.15

According to the Table-1, the distance of the coil is 1 cm to center of loop current, when the train comes from, for example 38,35 cm/s, the wemos can only read a few signal values. The distance from the coil to the center of the loop must be adjusted to optimize the sensor reading.

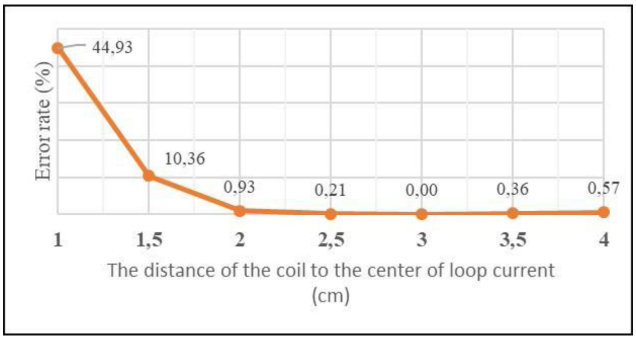

Figure-13. Error rate based on distance of the coil to the center of loop current and 100% PWM or 59, 78 cm/s speed of the train.

From the Figure-13 the train drove past 1400 crossing points. When the distance below 3 cm the error rate that shows is the number of crossing points that does not count as crossing point at it should be and when the distance above 3 cm the error rate that shows is the number of crossing points which is read at least twice on the crossing point. According to the table, the minimum distance of the coil to the center of the current loop to read all the crossing points until the maximum value of PWM is 3 cm. By using this minimum distance of the coil all the crossing points can be read but the problem is this distance is for maximum of PWM, when the train traveling below the maximum of PWM some crossing points read twice or more that's why the data need to filter so it's only selected once on every crossing point. The result of this implementation can see in Table-2.

Table-2. Success rate of crossing point when the distance of the coil to center of the loop current is 3cm.

No	PWM (%)	Speed (cm/s)	Speed in real life (km/h)	Total crossing points	Success rate (%)
1.	10	4,61	14,45	1400	100
2.	20	11,20	35,08	1400	100
3.	30	17,71	55,47	1400	100
4.	40	24,68	77,31	1400	100
5.	50	31,41	98,39	1400	100
6.	60	38,35	120,11	1400	100
7.	70	43,81	137,21	1400	100
8.	80	49,72	155,73	1400	100
9.	90	58,85	175,42	1400	100
10.	100	59,78	187,22	1400	100

Table-2 shows that the success rate is 100% to all the train speeds which is from 4, 61 cm/s to 59, 78 cm/s or in real life is 14, 45 km/h to 187, 22 km/h, which calculated based on 1:87 ratio of train miniature.

The wayside equipment using RFID to calibrate the position of trains, the reader placed at side of track and the tag placed on the side of train as show in Figure-14.

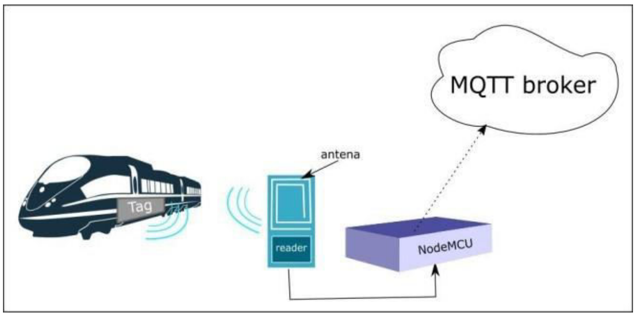

Figure-14. Wayside equipment illustration.

Base on Figure-14 when the train traveling right in front of the RFID reader, the reader will read the information of tag's train, the information will send to the MQTT broker so the server can analyze all the information from electromagnetic sensor and RFID. After all the information analyze the server can exactly know where all the trains traveling at while maintaining a safe distance.

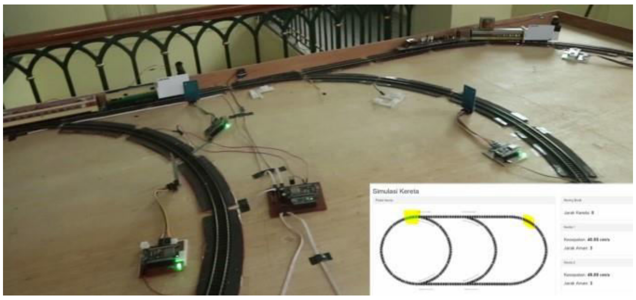

Figure-15. Implementation of moving block on train miniature.

The Figure-15 shows two trains traveling on the track, the distance of the two trains is 8 blocks, the train in front traveling at 40, 85 cm/s with safety braking distance is 3 blocks and the train behind traveling at 49, 89 cm/s with safety braking distance is also 3 blocks. When the distance is equal or below the safety distance the train behind will be slowing down then move faster again after the distance is longer than the safety distance. By using this simple rule all the trains can move closer to each other without any problem while keep maintains a safety distance separation.

CONCLUSIONS

The conclusion of this implementation and testing is the information of crossing point is just a sequence number based on how many crossing points that have been passed by train. Therefore, need to add one more device as a checkpoint to calibrate the position of the train on the rail track. The communication service playing as an important role in this to make sure that all the information's are sent in real-time and reliable.

REFERENCES

Indonesia's national rail network aims for more growth, less inequality, SE Asia News & Top Stories - The Straits Times.

Straitstimes. 2017. [Online]. Available: https://www.straitstimes.com/asia/se-asia/aim-more-growth-lessinequality. [Accessed: 16-Aug-2018].

A. Naeem M. 2015. Moving Block vs Fixed Block Signalling - Which is Better? | Naeem M Ali, P. Eng | Pulse | LinkedIn. Linkedin, 2015. [Online]. Available: https://www.linkedin.com/pulse/moving-blockvs-fixed-signalling-which-better-naeem-ali. [Accessed: 20-Aug2018].

M. T. H. Baheshti and M. H. M. Baygi. 2003. A Comparison Study of Fixed and Moving-Block Signalling in Rapid Transit Railways, Modares J. Electr. Eng. 3(1): 104-112.

N. M. Ali. 2018. What is CBTC? (IEEE 1474.1), Linkedin, 2015. [Online]. Available: https://www.linkedin.com/pulse/what-cbtc-ieee14741-naeem-ali. [Accessed: 14-Aug-2018].

Yuan Cao, Ru Niu, Tianhua Xu, Tao Tang and Jiancheng Mu. 2007. Wireless test platform of Communication Based Train Control (CBTC) system in urban mass transit. in 2007 IEEE International Conference on Vehicular Electronics and Safety. pp. 1-4.

J. Pochet, S. Baro and G. Sandou. 2016. Supervision and rescheduling of a mixed CBTC traffic on a suburban railway line. in 2016 IEEE International Conference on Intelligent Rail Transportation (ICIRT). pp. 32-38.

Khalifa Othman, Z a Obaid M, W b Naji A and Daoud Jamal. 2011. A rule-based Arabic Text-To-Speech system based on hybrid synthesis technique. Australian Journal of Basic and Applied Sciences. 5. 342-354.

X. Zhao, T. Tang and F. Yan. 2009. A Functional Safety Analysis Approach for Analyzing CBTC System. in 2009 International Conference on Measuring Technology and Mechatronics Automation. pp. 737-741.

J. Volinski. 2018. Reflections on the Future of Public Transportation. J. Public Transp. 21(1).

F. J. Sirait. 2017. Sistem Perangkat Keras dan Dashboard Kereta Pada Prototype Sistem Persinyalan Moving Block Kereta Api. Institut Teknologi Bandung.

N. R. Sree Harsha. 2016. Electromagnet induction. in The Foundations of Electric Circuit Theory, IOP Publishing.

T. Changqing, Z. Guoxin and R. Yanrong. 2009. Propagation in Tunnelin Case of WLAN Applied to Communications - Based Train Control System. Wirel. Mob. Comput. (CCWMC 2009), IET Int. Commun. Conf. pp. 393-396.

J. Farooq and J. Soler. 2017. Radio Communication for Communications-Based Train Control (CBTC): A Tutorial and Survey. IEEE Commun. Surv. Tutorials. 19(3): 1377-1402.